



RESEARCH ARTICLE

Altered multimodal magnetic resonance parameters of basal nucleus of Meynert in Alzheimer's disease

Weimin Zheng^{1,a}, Hui Li^{2,a}, Bin Cui¹ , Peipeng Liang³, Ye Wu¹, Xu Han¹, Chiang-shan R. Li^{4,5}, Kuncheng Li⁶ & Zhiqun Wang¹ 

¹Department of Radiology, Aerospace Center Hospital, Beijing, 100049, China

²Department of Radiology, Chaoyang Hospital of Capital Medical University, Beijing, 100020, China

³School of Psychology, Capital Normal University, Beijing Key Laboratory of Learning and Cognition, Beijing, 100037, China

⁴Department of Psychiatry, Yale University School of Medicine, New Haven, Connecticut

⁵Department of Neuroscience, Yale University School of Medicine, New Haven, Connecticut

⁶Department of Radiology, Xuanwu Hospital of Capital Medical University, Beijing, 100053, China

Correspondence

Zhiqun Wang, Department of Radiology, Aerospace Center Hospital, Haidian district, Beijing, 100049, China. Tel: +86-10-59972387; Fax: +86-10-59972425; E-mail: wangzhiqun@126.com

Funding Information This work was supported by the National Natural Science Foundation of China (Grant Nos. 81571648 and 81873892), Dongfang Hospital of Beijing University of Chinese Medicine, Independent Selection Project (No. 2018-JYBZZ-JS124) and Aerospace Center Hospital Youth Innovation Fund (No. 2020QN03), scientific research fund of Aerospace Center Hospital (No. YN201901), scientific research fund of China Aerospace Science & Industry Corp (No. 2019-LCYL-010), and the USA NIH grant (No. AG067024).

Received: 12 May 2020; Revised: 12 August 2020; Accepted: 19 August 2020

Annals of Clinical and Translational Neurology 2020; 7(10): 1919–1929

doi: 10.1002/acn3.51176

^aThe authors contributed equally to this work.

Introduction

Alzheimer's disease (AD) is a progressive neurodegenerative condition characterized by cognitive decline and memory deficit. Many animal and human studies have suggested the importance of acetylcholine in cognition, specifically in the modulation of information

Abstract

Objectives: We aimed to examine how gray matter volume (GMV), regional blood flow (rCBF), and resting-state functional connectivity (FC) of the basal nucleus of Meynert (BNM) are altered in 40 patients with AD, relative to 30 healthy controls (HCs). **Methods:** We defined the BNM on the basis of a mask histochemically reconstructed from postmortem human brains. We examined GMV with voxel-based morphometry of high-resolution structural images, rCBF with arterial spin labeling imaging, and whole-brain FC with published routines. We performed partial correlations to explore how the imaging metrics related to cognitive and living status in patients with AD. Further, we employed receiver operating characteristic analysis to compute the “diagnostic” accuracy of these imaging markers. **Results:** AD relative to HC showed lower GMV and higher rCBF of the BNM as well as lower BNM connectivity with the right insula and cerebellum. In addition, the GMVs of BNM were correlated with cognitive and daily living status in AD. Finally, these imaging markers predicted AD (vs. HC) with an accuracy (area under the curve) of 0.70 to 0.86. Combination of BNM metrics provided the best prediction accuracy. **Conclusions:** By combining multimode MR imaging, we demonstrated volumetric atrophy, hyperperfusion, and disconnection of the BNM in AD. These findings support cholinergic dysfunction as an etiological marker of AD and related dementia.

acquisition, encoding, consolidation, and retrieval.^{1–4} The basal forebrain cholinergic system may be impacted by pathological deposition of amyloid- β plaques and neurofibrillary tangles,⁵ contributing to memory and cognitive deficits in AD.^{6–8} Furthermore, cholinesterase inhibitors showed efficacy in improving cognitive functions in patients with AD.⁹ Thus, cholinergic deficiency

may represent a useful etiological marker of cognitive decline in AD.

The basal nucleus of Meynert (BNM) provides the major cholinergic inputs to the cerebral cortex and over 90% of BNM neurons are cholinergic.¹⁰ The BNM is “interdigitated” with several other anatomical structures of the basal forebrain, including the ventral pallidum as well as the nucleus accumbens, which has hampered precise anatomical delineation of the BNM in previous studies. In a recent work of cytoarchitectonics of postmortem human brains, Zaborszky and colleagues constructed a stereotaxic probabilistic map of the basal forebrain areas,¹¹ including the BNM. Previous studies have reported a reduction of BNM volume in patients with AD, including early stage AD,^{12–15} as compared with healthy controls (HCs). Furthermore, volumetric reduction of the BNM was associated with cognitive deficits in patients with early stage AD.¹⁶ The structural imaging studies provide potential evidence for cholinergic circuit dysfunction in AD and related dementia.

Resting-state functional magnetic resonance imaging (rs-fMRI) has proven to be a highly effective method in investigating neural circuit connectivities.^{17–19} Numerous rs-fMRI studies have demonstrated disrupted functional connectivity (FC) within the default mode,^{18,20–22} executive control,²³ and salience^{24–26} networks in AD. As the most important component of the basal forebrain cholinergic system,²⁷ the BNM circuit may interact with a wide array of brain regions to support attention and cognitive functions. With the stereotaxic map of the BNM constructed by Zaborszky and colleagues, previous rs-fMRI studies described whole-brain BNM connectivities in healthy people²⁸ as well as in smokers as compared to nonsmokers.²⁹ Another study employed electroencephalography to characterize the roles of cholinergic projections in the reactivity of alpha frequency band during transition from “eyes closed” to “eyes opened.”³⁰ Two recent studies also focused on the BNM network to delineate cholinergic deficits in AD and early stage AD, each showing disconnection between the BNM and insula/claustum in association with cognitive impairments³¹ and BNM network metrics predicting treatment response to cholinesterase inhibition.³² These findings shed light on cholinergic circuit functions in humans and provide important data to support the cholinergic bases of cognitive dysfunction during healthy aging and in the development of AD.

The integrity of regional brain function has also been investigated with the measures of cerebral blood flow (rCBF).³³ Arterial spin labeling (ASL) MRI provides quantitative information of rCBF. A recent meta-analysis revealed decreases in rCBF in the bilateral posterior cingulate cortex and precuneus, bilateral inferior parietal lobule, and left dorsolateral prefrontal cortex in patients with AD.³⁴ No studies have examined whether rCBF is

disrupted in the BNM regions or how altered rCBF may relate to changes in gray matter volume (GMV), functional activity or connectivity of the BNM in AD.

In this study, we aimed to identify the differences in the GMV, rCBF, and FC of the BNM in patients with AD relative to HCs. To this end, we will employ voxel-based morphometry (VBM) to examine GMV and ASL to examine rCBF, and explore resting-state FC of the BNM. Furthermore, we investigated the relationship between cognitive and living status and these imaging measures. Finally, on the basis of these imaging findings, we employ receiver operating characteristic (ROC) analysis to differentiate patients with AD and HC, in search for the best imaging biomarkers of AD. We hypothesize that: 1) the BNM region would show decreases in GMV, rCBF, and FC in patients with AD relative to HC; 2) altered imaging metrics of the BNM are associated with cognitive deficits in AD; and 3) the imaging markers would have significant sensitivity and specificity in the “diagnosis” of AD.

Materials and Methods

Subjects and assessments

Seventy subjects, including 40 patients with AD (46–92 years of age; 18 men) and 30 HCs (48–83 years of age; 15 men), participated in the study after providing written informed consent, in accordance with a protocol approved by the Medical Research Ethics Committee of Xuanwu Hospital, and the Declaration of Helsinki. All participants were right-handed. Patients with AD were recruited from the memory clinics at Xuanwu Hospital and HCs from the local community. The diagnosis of AD fulfilled the new research criteria for possible or probable AD.^{35,36} HCs met the following criteria: a) no neurological or psychiatric disorders such as stroke, depression, and epilepsy; b) no neurological deficiencies such as visual or hearing loss; c) no abnormal findings such as infarction or focal lesion in conventional brain MRI; d) no cognitive complaints; and e) CDR score of 0. Participants with contraindications for MRI such as having a pacemaker, cardiac defibrillator, implanted material with electric or magnetic system, vascular clips or mechanical heart valve, cochlear implant or claustrophobia were excluded. In addition, patients with a history of stroke, psychiatric diseases, drug abuse, uncontrolled hypertension, systematic diseases, and documented intellectual disability were excluded.

All participants underwent a complete physical and neurological examination, standard laboratory tests, and neuropsychological assessment. The assessment included the mini-mental state examination (MMSE),³⁷ activity of daily living scale (ADL),³⁸ clinical dementia rating (CDR) scale,³⁹ Hamilton Depression Scale (HAMD),⁴⁰ and Hamilton anxiety scale (HAMA).⁴¹ We employed a

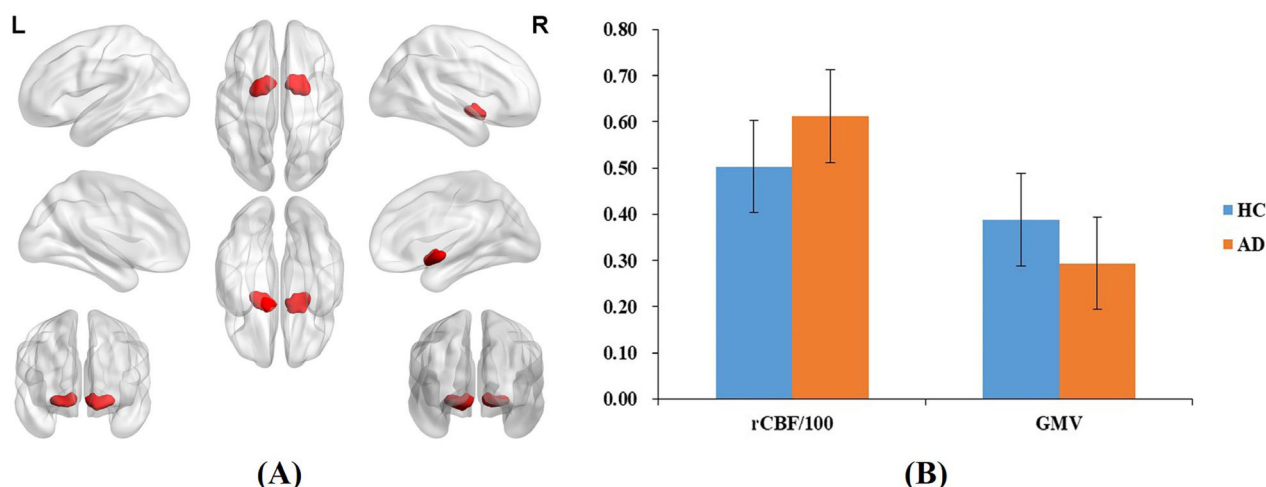


Figure 1. (A) The mask of the basal nucleus of Meynert (BNM). (B) Patients with AD showed significantly lower GMV ($P = 0.000$) and higher rCBF ($P = 0.005$) in the BNM, as compared with HCs. The y-axis means the gray matter volume and one hundredth of regional cerebral blood flow.

Chinese version of the ADL scale, with a total of 20 questions and each scored 1 to 4 – 1: can do by myself; 2: a little difficult but can do by myself; 3: need help to do it; and 4: cannot do it at all. The total score ranges from 20 to 80, with a higher score indicating more significantly compromised activity of daily living.

Imaging data acquisition

MRI data were acquired on a SIEMENS 3-Tesla scanner (Siemens, Erlangen, Germany). The subjects were instructed to hold still and keep eyes closed but not to fall asleep. 3D magnetization-prepared rapid gradient echo (MPRAGE) sagittal images were obtained with following parameters: TR/TE/inversion time (TI)/FA = 1900 ms/2.2 ms/900 ms/9°, image matrix = 256 × 256, slice number = 176, thickness = 1 mm. ASL data were acquired using the following parameters: TI/TI1 = 1.2s/700 ms, TR/TE = 2.0 s/14ms, FOV = 256 × 256 mm², matrix size = 64×64, in plane resolution = 3×3 mm², bandwidth = 2232Hz/px, phase partial Fourier = 6/8, EPI factor = 64. Twelve slices of 6-mm thickness were acquired. The resting-state fMRI data were acquired axially using an echo-planar imaging (EPI) with following parameters: repetition time (TR)/echo time (TE)/flip angle (FA)/field of view (FOV) = 2000 ms/40 ms/90°/24 cm, image matrix = 64×64, slice number = 33, thickness = 3 mm, gap = 1 mm, bandwidth = 2232 Hz/pixel, with one 6-minute scan per subject.

Imaging data processing

We computed the GMV, regional cerebral blood flow, and whole-brain FC of the BNM using the mask of Zaborszky et al.¹¹ (Figure 1A).

Voxel-based morphometry (VBM) analysis

The structural data preprocessing was performed using Statistical Parametric Mapping (SPM8) software (<http://www.fil.ion.ucl.ac.uk/spm/>), as implemented in MATLAB 2013a (Math Works, Natick, MA, USA). First, all images were manually reoriented to place the anterior commissure at the origin and the anterior–posterior commissure in the horizontal plane. Second, images were segmented into gray matter (GM), white matter (WM), and cerebrospinal fluid (CSF) areas, using the unified standard segmentation option in SPM8. Third, individual WM and GM components were normalized into the standard Montreal Neurological Institute (MNI) space using the Diffeomorphic Anatomical Registration through Exponentiated Lie algebra (DARTEL) algorithm.⁴² The normalized GM and WM components were modulated to generate the relative GMV and white matter volume (WMV) by multiplication by the nonlinear part of the deformation field. Fourth, the resulting GMV and WMV images were smoothed with an 8-mm full width at half maximum (FWHM) Gaussian kernel. Finally, the GMVs of BNM were calculated for each subject using REST V1.82⁴³ software (in MATLAB) for subsequent statistical analysis.

Arterial spin labeling (ASL) data analysis

ASL data were analyzed using custom MATLAB (The Mathworks Inc., Natick, MA) scripts and ASL toolbox.⁴⁴ The rCBF images were normalized to the MNI space using the following steps: (1) Data were converted from EPI digital imaging and communications in medicine (DICOM) to neuroimaging informatics technology initiative (NIFTI) format with the orientation

and origin reset; (2) Functional images were realigned to the first volume (M0); M0 was registered to the mean blood oxygen level-dependent (BOLD) image generated during motion correction for the raw ASL images; functional images were then coregistered to the anatomical image; mean rCBF maps were normalized in MNI space; during this procedure, partial volume effect (PVE) correction was performed to correct rCBF at each voxel in the GM. (3) The coregistered functional images were smoothed by an isotropic Gaussian kernel with FWHM at 4 mm; (4) Batch calculation for the perfusion signals; and (5) The CBF of the BNM was calculated for individual subjects using REST V1.82⁴³ software for subsequent statistical analyses.

Functional connectivity (FC) analysis

The functional data processing was performed using the Data Processing Assistant for Resting-State fMRI⁴⁵ (DPARF, <http://rfmri.org/DPARF>). The procedure included the following: (1) The first 10 volumes were removed; (2) Slice timing and head motion correction; subjects with maximum head movements >2 mm in translation or >2° in rotation were excluded; (3) The realigned volumes were spatially normalized in the MNI space using the EPI template, and the functional images were resampled into a voxel size of 3 × 3 × 3 mm³; (4) The data were smoothed with a Gaussian filter of 4-mm FWHM to reduce noise and residual differences in gyral anatomy; (5) Regress out the Friston-24 parameters, their first time-derivatives, and global, WM, and CSF signals; (6) Time band-pass filtering (0.01–0.08 Hz) was performed to reduce the effects of a low-frequency drift and high-frequency physiological noise; (7) FC of the BNM was computed by voxel-wise correlation between the time series of the BNM and of the entire brain; and (8) Regions of interest (ROI) were defined by group differences and the FC of the ROIs were calculated using REST V1.82⁴³ for individual subjects.

Statistical analyses

We performed independent-samples *t*-tests to assess the between-group differences (AD vs. HC) in the GMV and rCBF of the BNM with age, gender, and education level as covariates.

Then, two-sample *t* test was performed with age, gender, and education level as covariates to analysis the FC changes between AD and HCs using Statistical Parametric Mapping software package (SPM8, <http://www.fil.ion.ucl.ac.uk/spm>). The significance threshold was set to false discovery rate (FDR) correction (cluster-wise, $P < 0.05$). In order to reduce the impact of GMV atrophy on FC, we also analyzed the BNM-FC changes with age, gender, education level, and

GMV as covariates (voxel $P < 0.001$, uncorrected, in combination with cluster-level $P < 0.05$, FDR corrected).

To explore the associations of the clinical variables with the GMV, rCBF, and FC in the patients with AD, partial correlation analysis were performed with age, gender, and education being used as nuisance covariates ($P < 0.05$, SPSS20.0).

Finally, we used ROC analysis with SPSS20.0 to compute the sensitivity and specificity of the imaging biomarkers for AD diagnosis. The ROC analysis essentially employed a binary classifier of AD vs. HC as the discrimination threshold was varied from high to low. We created the ROC curve by plotting the true positive rate against the false positive rate at various thresholds. We performed the ROC curve of the GMV, rCBF, and FC of the BNM, respectively, and the optimal two combined values (BNM connectivity with the left cerebellum and right insula).

Results

Demographic and neuropsychological tests

Demographic characteristics are shown in Table 1. There are no significant group differences in years of age, gender composition, and years of education (all P 's > 0.46). The AD group showed significantly lower MMSE and higher ADL scores than the HC group (P 's < 0.001).

Gray matter volume (GMV) and regional cerebral blood flow (rCBF) of the BNM

Independent-samples *t*-tests demonstrated that patients with AD relative to HC showed significantly lower GMV

Table 1. Clinical and demographical data

	AD (n = 40)	HC (n = 30)	<i>p</i> -Value
Age (y)	65.1 ± 9.9	63.9 ± 7.5	0.46 ^a
Gender (male/ female)	18/22	15/15	0.51 ^b
Education (years)	11.6 ± 7.3	11.4 ± 3.2	0.93 ^a
CDR	CDR = 1(22)/ CDR = 2(18)	0	-
MMSE	4-24 (14.2 ± 5.5)	21-30 (26.9 ± 3.0)	<0.001 ^a
ADL	20-60 (29.11 ± 8.35)	20-21 (20.07 ± 0.25)	<0.001 ^a
HAMD	0-13 (2.34 ± 3.12)	0-11 (1.97 ± 2.47)	0.597 ^a
HAMA	0-16 (4.74 ± 3.82)	0-10 (3.03 ± 2.69)	0.045 ^a

Data are shown as range (mean ± SD).

AD, Alzheimer's disease; HC, healthy controls; CDR, Clinical Dementia Rating; MMSE, Mini-Mental State Examination; ADL, Activity of Daily Living Scale; HAMD, Hamilton Depression Scale; HAMA, Hamilton anxiety scale; a, two-sample two-tailed *t*-test; b, two-tailed Pearson chi-squared test.

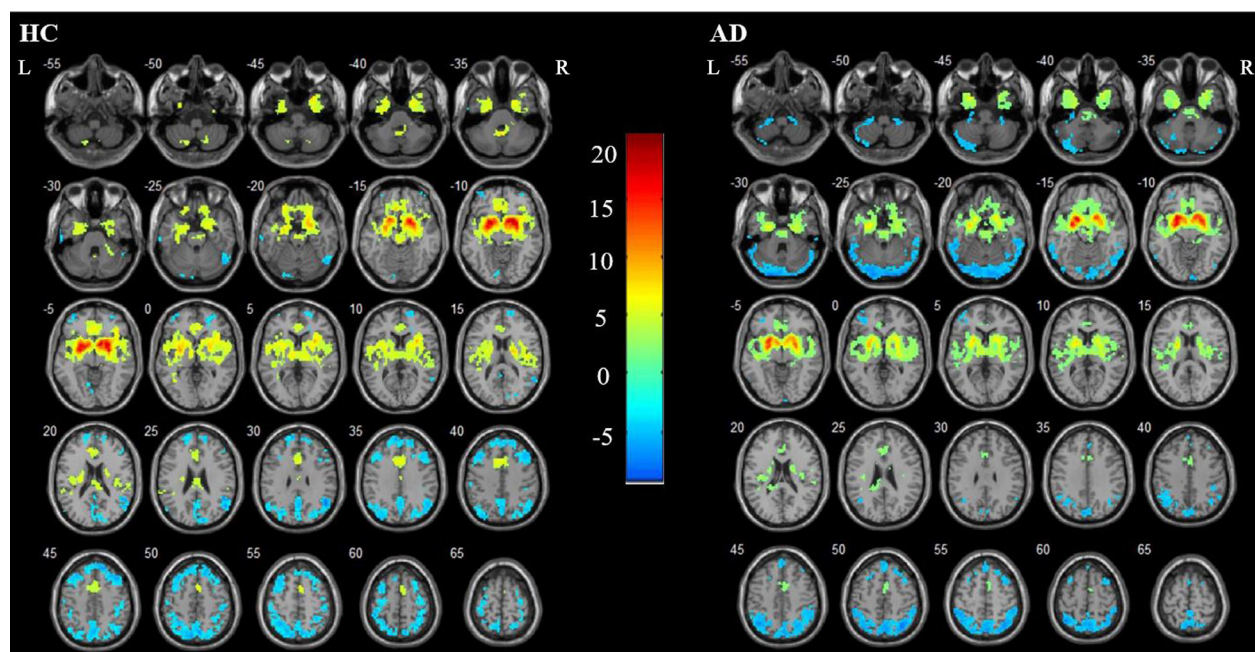


Figure 2. Whole-brain functional connectivity of the basal nucleus of Meynert (BNM) in healthy controls (HCs) and patients with Alzheimer's disease (AD). The results were thresholded at voxel-wise $P < 0.001$, uncorrected. The color scale means T-scores.

(0.29 ± 0.07 vs. 0.39 ± 0.06 ; $t = -5.082$, $P = 0.000$) and higher rCBF (61.26 ± 19.41 vs. 50.34 ± 11.05 ; $t = 3.176$, $P = 0.002$) in the BNM (Figure 1B).

Whole-brain functional connectivity (FC) of the BNM

Within-group analysis revealed both positive and negative FC of the BNM with many brain regions in HCs as well as in patients with AD. The BNM showed positive connectivity with the orbitofrontal cortex, temporal cortex, medial frontal cortex, including the ventromedial prefrontal and anterior cingulate cortices and supplementary motor area, bilateral hippocampi, amygdala, thalamus, insula, and basal ganglia. The BNM showed negative connectivity with a large swath of occipital, frontoparietal, and frontopolar cortices (Figure 2). These findings largely replicated a previous report of whole-brain BNM-FC in a larger sample.²⁸

We compared patients with AD and HC in BNM connectivities in a two-sample t test for the whole brain. The results showed that, relative to HC, patients with AD showed less BNM connectivity with the left cerebellum ($x = -18$, $y = -69$, $z = -51$, $Z = -4.9051$, 49 voxels) and right insula ($x = 42$, $y = 24$, $z = 0$, $Z = -4.8811$, 80 voxels) at the same threshold: voxel $P < 0.001$, uncorrected, in combination with cluster-level $P < 0.05$, FDR corrected (Figure 3).

In order to reduce the impact of GMV atrophy on FC, we also analyzed the BNM-FC changes after GMV correction, and found that relative to HC, patients with AD showed less BNM connectivity with the left cerebellum (voxel $P < 0.001$, uncorrected, in combination with cluster-level $P < 0.05$, FDR corrected), which was similar to the result above.

Correlations of imaging findings with cognitive status

We observed lower GMV and higher rCBF of the BNM as well as lower FC of the BNM with the left cerebellum and right insula. Thus, we examine how these four imaging measure may correlate with the MMSE and ADL scores in patients with AD. Because MMSE and ADL scores were correlated ($r = -0.369$, $P = 0.029$), we evaluated these regressions with a corrected p value of $0.05/4$ (four neural measures) = 0.0125. The results showed that the GMV of BNM was trend-correlated with MMSE score ($r = 0.373$, $P = 0.023$) and significantly correlated with ADL score ($r = -0.461$, $P = 0.004$) (Figure 4). In addition, we made the partial correlation analysis among the three measures. In the result, we did not find significant correlation between the rCBF and GMV in BNM, or rCBF in BNM, and BNM-FC, but we found significantly positive correlation between GMV in BNM and BNM-FC with right insula ($r = 0.388$, $P = 0.028$).

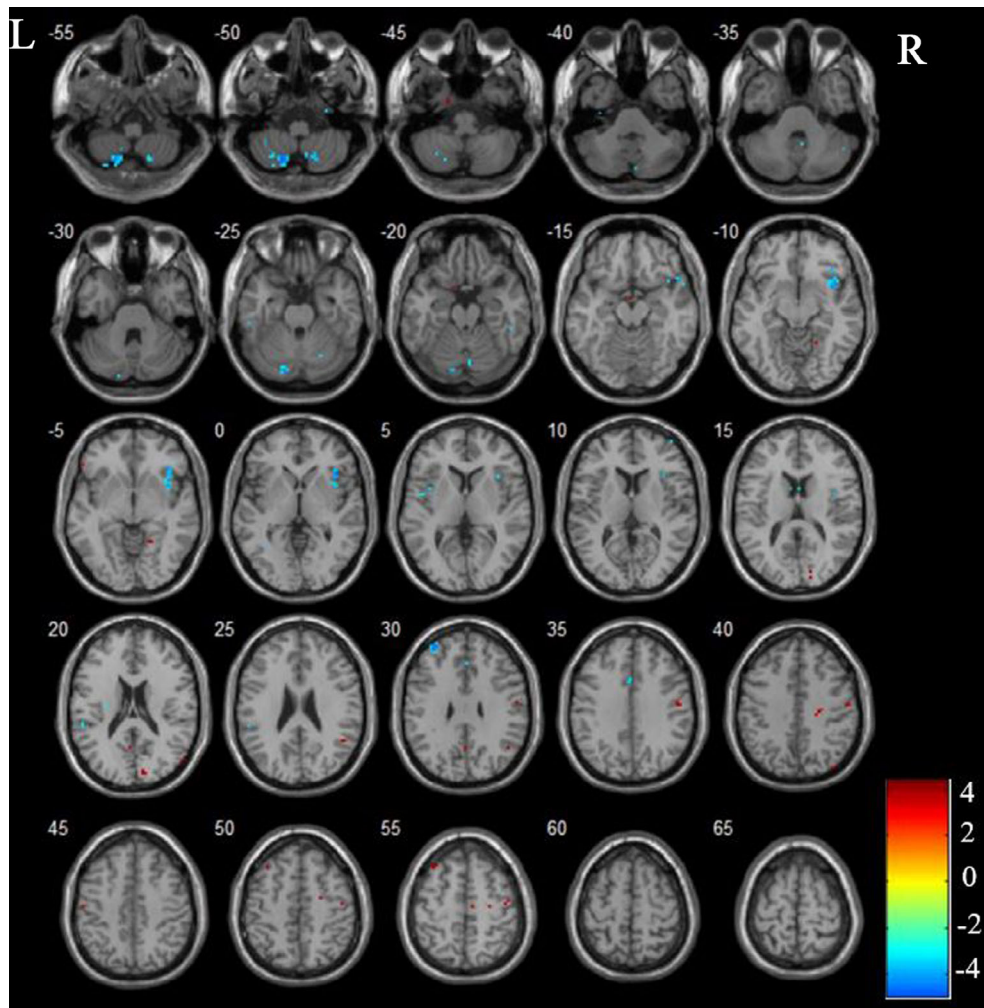


Figure 3. Decreased BNM-left cerebellum/right insula connectivity in patients with AD. AD, Alzheimer’s disease. Two-sample t test: voxel $P < 0.001$, uncorrected, in combination with cluster $P < 0.05$ FDR corrected. The color scale means T-scores: warm: AD>HC; cool: AD<HC.

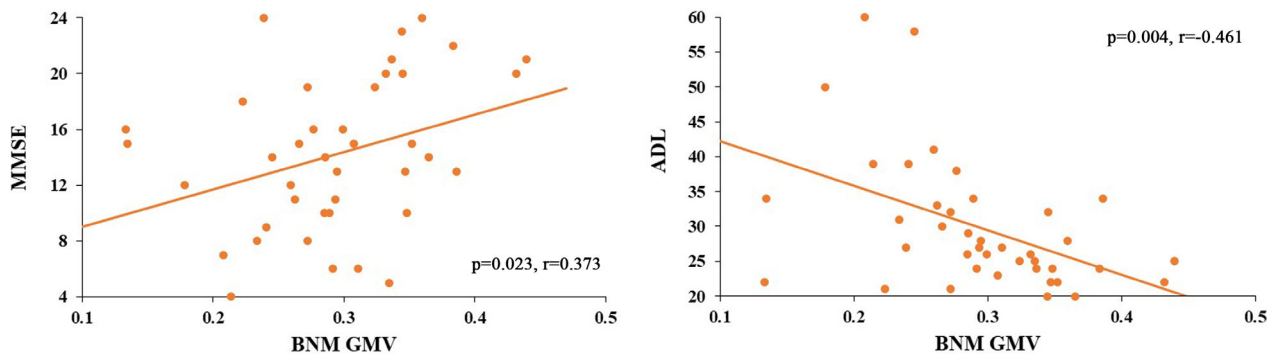


Figure 4. Linear correlation of the mini-mental state examination (MMSE) and activity of daily living scale (ADL) scores with the gray matter volumes of the BNM in patients with AD.

Table 2. Area under the curve (AUC) of the GMV, rCBF, and FC in the “diagnosis” of AD

Test Result Variable(s)	AUC	SE	Asymptotic 95% Confidence Interval P value ^a	Asymptotic 95% Confidence Interval	
				Lower Bound	Upper Bound
GMV	0.838	0.053	0.000	0.735	0.942
rCBF	0.703	0.067	0.007	0.573	0.834
FC (Insula)	0.851	0.051	0.000	0.752	0.950
FC (Cerebellum)	0.859	0.046	0.000	0.769	0.950
Combined FC	0.951	0.030	0.000	0.892	1.009

GMV, gray matter volume; rCBF, regional cerebral blood flow; FC, functional connectivity; BNM, basal nucleus of Meynert; SE: standard error.

a. Null hypothesis: true area = 0.5.

ROC analysis of neural measures as a biomarker of AD

The BNM showed significant differences in GMV, rCBF, and resting-state FC in patients with AD relative to HCs, raising the possibility that these neural measures may serve as biomarkers of AD. We employed ROC analysis to explore the issue. The area under the curve (AUC) of the GMV, rCBF, and FC values in BNM was 0.838, 0.703, 0.851, and 0.859 respectively (Table 2 and Figure 5A). Figure 5B shows the sensitivity and specificity of the BNM-FC of the left cerebellum and right insula in combination, with a sensitivity of 92.3%, specificity of 94.3%, and AUC of 0.951 (95% confidence intervals: 0.892 to 1.009).

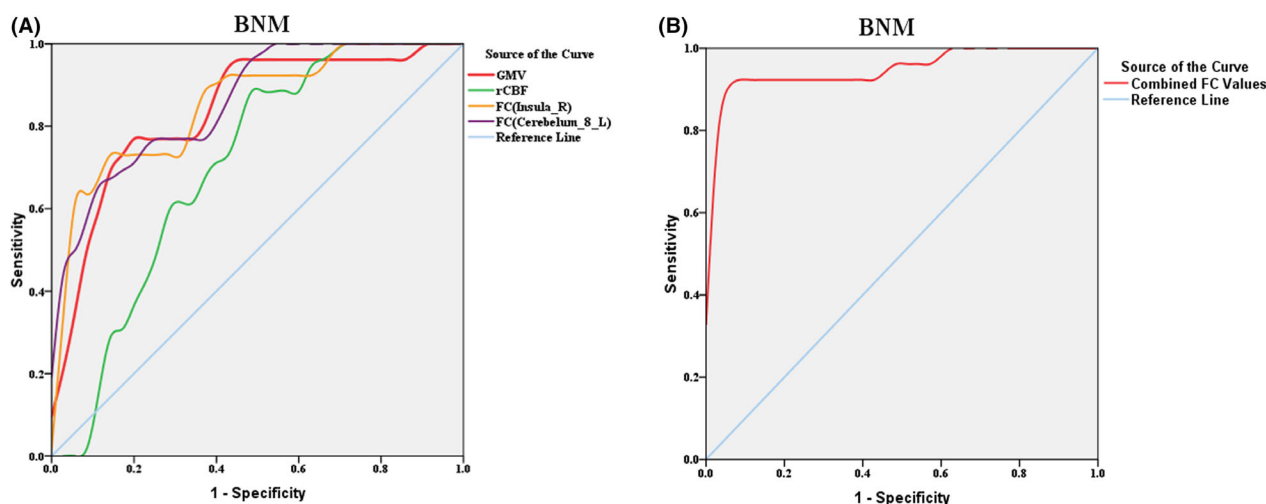


Figure 5. (A) Receiver operating characteristic (ROC) curve of the GMV, rCBF, and FC of the BNM. The AUC for the ROC was 0.838, 0.703, 0.851, and 0.859 respectively. (B) ROC curve for the BNM-FC with left cerebellum and right insula in combination. An optimal combined FC cutoff value was determined at a sensitivity of 92.3% and specificity of 94.3%. The AUC for the ROC was 0.951 (95% confidence intervals from 0.892 to 1.009). GMV, gray matter volume; rCBF, regional cerebral blood flow; FC, functional connectivity; BNM, basal nucleus of Meynert.

Discussion

To our knowledge, this is the first study to investigate how the GMV, rCBF, and FC of the BNM are altered in AD. We found decreases in GMV, increases in rCBF of BNM, and decreases in BNM connectivity with the cerebellum and insula in patients with AD relative to controls. Greater changes in the GMV were associated with diminished cognitive and daily living status in patients with AD. Further, the ROC analyses demonstrated that the combination of BNM-FC of left cerebellum and right insula could best differentiate AD from controls. Together, these findings support cholinergic dysfunction as an important etiological mechanism of AD.

Altered GVM and rCBF of the BNM in AD

Replicating previous studies,^{11-15,44} we found decreased GMV of the BNM in patients with AD. Many imaging studies have demonstrated atrophy of the BNM during healthy aging⁴⁵ and in individuals with MCI^{11,13,44} or AD.^{12,14,15} These findings are consistent with neuronal loss in the BNM during the early stage of AD.⁴⁶ With the development of the disease, volumetric reduction extended from the BNM to the whole basal forebrain, in association with deterioration in cognitive status.^{13,16} Indeed, we showed that BNM GMV was associated with cognitive and living status each reflected by the MMSE and ADL score in patients with AD.

In the current study, we found the increased rCBF of BNM in the patients with AD relative to HCs. A majority of previous ASL studies have revealed cerebral

hypoperfusion in AD, mainly in the temporoparietal, frontal, and occipital cortex and basal ganglia.⁴⁷⁻⁴⁹ A recent voxel-wise meta-analysis reported decreases in rCBF in the posterior cingulate cortex/precuneus, inferior parietal lobule, and dorsolateral prefrontal cortex.³⁴ However, other studies showed hyperperfusion in regions of the cognitive networks, which suggests compensatory or pathological elevation of neural activity, inflammation, or elevated production of vasodilators.⁵⁰⁻⁵⁴ In this study, increased rCBF may similarly reflect a compensation for volumetric reduction of the BNM.

Altered functional connectivity of the BNM

Previous study has mapped whole-brain functional connectivity of the BNM in neurotypical populations.²⁸ The BNM network, including key regions of the default mode and salience networks, as well as the bilateral caudate nuclei, largely overlapped with the anatomical cholinergic pathways.⁵⁵ Specifically, the medial cholinergic pathway connects the BNM with medial prefrontal cortices, anterior cingulate cortex, and subcortical regions. The lateral cholinergic pathway connects the BNM with bilateral hippocampi, insula, and other subcortical targets.

The current findings revealed disconnection between the BNM and right insula in patients with AD. The insula is a crucial hub of salience, executive control, and default mode networks⁵⁶⁻⁵⁸ and anatomically connected with many cortical, limbic, and paralimbic structures. The insula plays a critical role in a myriad of cognitive and affective processes.⁵⁹ Previous imaging studies have revealed insular atrophy,⁶⁰ disrupted insular activities⁶¹ and connectivities in early stage AD.^{62,63} A β plaques and neurofibrillary tangles have been consistently detected in the insula and BNM in AD.⁶⁴⁻⁶⁶ Importantly, recent studies have also reported functional disconnection between the BNM and insula, in close association with cognitive decline, in MCI patients.^{31,32} More studies are needed to examine the specific implications of BNM insula dysconnectivity for cognitive and affective functioning in AD and related dementia. In particular, the insula is central to the integration of emotion and cognition, and impaired insula function may lead to motivational dysfunction or apathy, which manifests early in the disease process of AD.⁶⁷⁻⁷⁰

We also found lower BNM cerebellum connectivity in patients with AD as compared to HC. Earlier studies have reported GM atrophy,^{71,72} lower CBF,⁷³ altered activation⁷⁴ and FC of the cerebellum^{21,75} in AD. Although rarely a focus, the cerebellum showed AD pathological changes including amyloid- β plaques and neurofibrillary tangles.^{76,77} In our recent study, we reported disrupted functional connectivity of cerebellar subregions in link with cognitive deficits in AD.⁷⁸ Likewise, more studies are

needed to evaluate the functional implication of BNM cerebellum dysconnectivity.

BNM metrics as markers of AD

We performed ROC analyses to characterize how the BNM metrics may serve as biomarkers of AD. Among the metrics, the combination of BNM insula and cerebellum FC provided the best sensitivity (92.3%) and specificity (94.3%). Further, using the combination metric, we were able to accurately differentiate the two groups at an AUC of 0.951, suggesting that combination of FC features of the BNM could provide a most valuable biomarker for the diagnosis of AD.

Limitations of the study and conclusions

Several limitations should be considered. First, this is a cross-sectional study with a moderate sample size. Longitudinal studies of a larger cohort are needed to reveal how the structural and functional changes of the BNM would evolve as the disease progresses. Likewise, studies of patients with amnesic mild cognitive impairments (aMCI) and early stage AD and of ApoE-4 allele carriers would elucidate the role of the cholinergic circuit dysfunction in the onset and etiological processes of the disease. Second, the current participants were not evaluated with neurocognitive tasks and we were not able to relate these BNM metrics to cognitive and affective functions in more detail. In the future we will collect more neuropsychological tests such as CDT, AVLT, MoCA, and so on, exploring the relationship among the BNM atrophy, global atrophy, and different tests. Finally, in the current study, the data of participants were normalized to MNI152. Future studies involving Chinese populations should be considered to normalize to Chinese 2020 (a typical statistical Chinese brain template).

Furthermore, cholinergic deficiency may represent a useful etiological marker of cognitive decline in AD. There are some clinical biomarkers to directly reflect the cholinergic deficiency such as acetylcholine content in CSF. Establishing relationship among acetylcholine level and dementia degree, as well as Meynert imaging would be valuable to provide the new evidence for the mechanisms of AD. However, CSF measurement is an invasive examination, which has certain risks. In the future we will try our best to overcome these challenges to collect more clinical information.

Overall, our results proved the atrophy, hyperperfusion, and disconnection of BNM in patients with AD. Within the current sample, the BNM imaging metrics, particularly BNM-FC with left cerebellum and right insula, could be a valuable biomarker for characterizing the intrinsic

brain organization and its integrity in patients with AD, potentially featuring higher sensitivity and specificity in detecting patients with AD from HCs.

Ethics Approval and Consent to Participate

This study was carried out in accordance with a research protocol approved by the Medical Research Ethics Committee of Xuanwu Hospital. All participants gave written informed consent prior to the study.

Conflicts of Interest

The authors declare that they have no conflict of interest.

Author' Contributions

ZQW, WMZ, and HL were responsible for the study concept and design. YW and XH contributed to the acquisition of MRI data. WMZ, HL, BC, and PPL assisted with data analysis and interpretation. WMZ, HL, and ZQW drafted the manuscript. CRL contributed to conceptualization of the study and revision of the manuscript. All the authors provided critical revision of the manuscript, reviewed the content, and approved the final version of the manuscript.

Acknowledgments

The authors thank the patients and their families for the time and effort they dedicated to the research. In addition, we are grateful to our colleague from Yale University School of Medicine.

Data Availability Statement

The raw/processed data during the study are proprietary and confidential, it cannot be shared at this time as the data also form part of an ongoing study.

References

- Blokland A, Honig W, Raaijmakers WG. Effects of intra-hippocampal scopolamine injections in a repeated spatial acquisition task in the rat. *Psychopharmacology* 1992;109:373–376.
- Boccia MM, Blake MG, Baratti CM, et al. Involvement of the basolateral amygdala in muscarinic cholinergic modulation of extinction memory consolidation. *Neurobiol Learn Mem* 2009;91(1):93–97.
- Power AE, Vazdarjanova A, McGaugh JL. Muscarinic cholinergic influences in memory consolidation. *Neurobiol Learn Mem* 2003;80:178–193.
- Winters BD, Bussey TJ. Removal of cholinergic input to perirhinal cortex disrupts object recognition but not spatial working memory in the rat. *Eur J Neurosci* 2005;21:2263–2270.
- Braak H, Braak E. Neuropathological staging of Alzheimer-related changes. *Acta Neuropathol* 1991;82:239–259.
- Mesulam MM, Volicer L, Marquis JK, et al. Systematic regional differences in the cholinergic innervation of the primate cerebral cortex: distribution of enzyme activities and some behavioral implications. *Ann Neurol* 1986;19:144–151.
- Ruberg M, Mayo W, Brice A, et al. Choline acetyltransferase activity and [³H]vesamicol binding in the temporal cortex of patients with Alzheimer's disease, Parkinson's disease and rats with basal forebrain lesions. *Neuroscience* 1990;35:327–333.
- Vogels OJM, Broere CA, Ter Laak HJ, et al. Cell loss and shrinkage in the nucleus basalis Meynert complex in Alzheimer's disease. *Neurobiol Aging* 1990;11:3–13.
- Richter N, Allendorf I, Onur OA, et al. The integrity of the cholinergic system determines memory performance in healthy elderly. *NeuroImage* 2014;100:481–488.
- Gratwicke J, Kahan J, Zrinzo L, et al. The nucleus basalis of Meynert: a new target for deep brain stimulation in dementia? *Neurosci Biobehav Rev* 2013;37:2676–2688.
- Zaborszky L, Hoemke L, Mohlberg H, et al. Stereotaxic probabilistic maps of the magnocellular cell groups in human basal forebrain. *NeuroImage* 2008;42:1127–1141.
- George S, Mufson EJ, Leurgans S, et al. MRI-based volumetric measurement of the substantia innominata in amnesic MCI and mild AD. *Neurobiol Aging* 2011;32:1756–1764.
- Grothe M, Heinsen H, Teipel SJ. Atrophy of the cholinergic basal forebrain over the adult age range and in early stages of Alzheimer's disease. *Biol Psychiatry* 2012;71:805–813.
- Grothe M, Heinsen H, Teipel S. Longitudinal measures of cholinergic forebrain atrophy in the transition from healthy aging to Alzheimer's disease. *Neurobiol Aging* 2013;34:1210–1220.
- Grothe MJ, Schuster C, Bauer F, et al. Atrophy of the cholinergic basal forebrain in dementia with Lewy bodies and Alzheimer's disease dementia. *J Neurol* 2014;261:1939–1948.
- Grothe M, Zaborszky L, Atienza M, et al. Reduction of basal forebrain cholinergic system parallels cognitive impairment in patients at high risk of developing Alzheimer's disease. *Cereb Cortex* 2010;20:1685–1695.
- Biswal B, Yetkin FZ, Haughton VM, et al. Functional connectivity in the motor cortex of resting human brain using echo-planar MRI. *Magn Reson Med* 1995;34:537–541.
- Zhang H, Wang S, Liu B, et al. Resting brain connectivity: changes during the progress of Alzheimer disease. *Radiology* 2010;256:598–606.

19. Raichle ME, MacLeod AM, Snyder AZ, et al. A default mode of brain function. *Proc Natl Acad Sci USA* 2001;98:676–682.
20. Greicius MD, Srivastava G, Reiss AL, et al. Default-mode network activity distinguishes Alzheimer's disease from healthy aging: evidence from functional MRI. *Proc Natl Acad Sci USA* 2004;101:4637–4642.
21. Wang K, Liang M, Wang L, et al. Altered functional connectivity in early Alzheimer's disease: a resting-state fMRI study. *Hum Brain Mapp* 2007;28:967–978.
22. Dai Z, Yan C, Wang Z, et al. Discriminative analysis of early Alzheimer's disease using multi-modal imaging and multi-level characterization with multi-classifier (M3). *NeuroImage* 2012;59:2187–2195.
23. Seeley WW, Crawford RK, Zhou J, et al. Neurodegenerative diseases target large-scale human brain networks. *Neuron* 2009;62:42–52.
24. Agosta F, Pievani M, Geroldi C, et al. Resting state fMRI in Alzheimer's disease: beyond the default mode network. *Neurobiol Aging* 2012;33:1564–1578.
25. Brier MR, Thomas JB, Snyder AZ, et al. Loss of intranetwork and internetwork resting state functional connections with Alzheimer's disease progression. *J Neurosci* 2012;32:8890–8899.
26. Wang Z, Xia M, Dai Z, et al. Differentially disrupted functional connectivity of the subregions of the inferior parietal lobule in Alzheimer's disease. *Brain Struct Funct* 2015;220:745–762.
27. Liu AK, Chang RC, Pearce RK, et al. Nucleus basalis of Meynert revisited: anatomy, history and differential involvement in Alzheimer's and Parkinson's disease. *Acta Neuropathol* 2015;129:527–540.
28. Li CR, Ide JS, Zhang S, et al. Resting state functional connectivity of the basal nucleus of Meynert in humans: in comparison to the ventral striatum and the effects of age. *NeuroImage* 2014;97:321–332.
29. Zhang S, Hu S, Fucito LM, et al. Resting-State functional connectivity of the basal nucleus of meynert in cigarette smokers: dependence level and gender differences. *Nicotine Tob Res* 2017;19(4):452–459.
30. Wan L, Huang H, Schwab N, et al. From eyes-closed to eyes-open: role of cholinergic projections in EC-to-EO alpha reactivity revealed by combining EEG and MRI. *Hum Brain Mapp* 2019;40(2):566–577.
31. Li H, Jia X, Qi Z, et al. Altered functional connectivity of the basal nucleus of meynert in mild cognitive impairment: a resting-state fMRI study. *Front Aging Neurosci* 2017;9:127.
32. Meng D, Li X, Bauer M, et al. Alzheimer's disease neuroimaging initiative. Altered nucleus basalis connectivity predicts treatment response in mild cognitive impairment. *Radiology* 2018;289(3):775–785.
33. Liang X, Zou Q, He Y, et al. Coupling of functional connectivity and regional cerebral blood flow reveals a physiological basis for network hubs of the human brain. *Proc Natl Acad Sci USA*. 2013;110:1929–1234.
34. Ma HR, Pan PL, Sheng LQ, et al. Aberrant pattern of regional cerebral blood flow in Alzheimer's disease: a voxel-wise meta-analysis of arterial spin labeling MR imaging studies. *Oncotarget* 2017;8:93196–93208.
35. Dubois B, Feldman HH, Jacova C, et al. Revising the definition of Alzheimer's disease: a new lexicon. *Lancet Neurol* 2010;9:1118–1127.
36. Dubois B, Feldman HH, Jacova C, et al. Research criteria for the diagnosis of Alzheimer's disease: revising the NINCDS-ADRDA criteria. *Lancet Neurol* 2007;6:734–746.
37. Folstein MF, Folstein SE, McHugh PR. "Mini-mental state". A practical method for grading the cognitive state of patients for the clinician. *J Psychiatr Res*. 1975;12:189–198.
38. Iijima S. Disability assessment for dementia (DAD), Alzheimer's Disease cooperative study-activities of daily living (ADCS-ADL). *Nihon rinsho Jpn J Clin Med* 2011;69(8):471–474.
39. Morris JC. The clinical dementia rating (CDR): current version and scoring rules. *Neurology* 1993;43:2412.
40. Leucht S, Fennema H, Engel R, et al. What does the HAMD mean? *J Affect Disord* 2013;148:243–248.
41. Hamilton M. The assessment of anxiety states by rating. *Br J Med Psychol*. 1959;32:50–55.
42. Ashburner J. A fast diffeomorphic image registration algorithm. *NeuroImage* 2007;38:95–113.
43. Song X, Dong Z, Long X, et al. REST: a toolkit for resting-state functional magnetic resonance imaging data processing. *PLoS One* 2011;6(9):e25031.
44. Wang Z, Aguirre GK, Rao H, et al. Empirical optimization of ASL data analysis using an ASL data processing toolbox: ASLtbx. *Magn Reson Imaging* 2008;26:261–269.
45. Yan C, Zang YF. DPARSF: aMATLAB toolbox for "pipeline" data analysis of resting-state fMRI. *Front Syst Neurosci* 2010;4:13.
46. Hanyu H, Asano T, Sakurai H, et al. MR analysis of the substantia innominata in normal aging, Alzheimer disease, and other types of dementia. *Am J Neuroradiol* 2002;23:27–32.
47. Kilimann I, Grothe M, Heinsen H, et al. Subregional basal forebrain atrophy in Alzheimer's disease: a multicenter study. *J Alzheimers Dis* 2014;40:687–700.
48. Arendt T, Brückner MK, Morawski M, et al. Early neurone loss in Alzheimer's disease: cortical or subcortical? *Acta Neuropathol Commun* 2015;3:10.
49. Vercllytte S, Lopes R, Lenfant P, et al. Cerebral hypoperfusion and hypometabolism detected by arterial spin labeling MRI and FDG-PET in Early-Onset Alzheimer's Disease. *J Neuroimaging*. 2016;26:207–212.
50. Zhang J. How far is arterial spin labeling MRI from a clinical reality? Insights from arterial spin labeling comparative studies in Alzheimer's disease and other

- neurological disorders. *J Magn Reson Imaging* 2016;43:1020–1045.
51. Alexopoulos P, Sorg C, Forschler A, et al. Perfusion abnormalities in mild cognitive impairment and mild dementia in Alzheimer's disease measured by pulsed arterial spin labeling MRI. *Eur Arch Psychiatry Clin Neurosci* 2012;262:69–77.
 52. Ding B, Ling HW, Zhang Y, et al. Pattern of cerebral hyperperfusion in Alzheimer's disease and amnesic mild cognitive impairment using voxel-based analysis of 3D arterial spin-labeling imaging: initial experience. *Clin Interv Aging* 2014;9:493–500.
 53. Roquet D, Sourty M, Botzung A, et al. Brain perfusion in dementia with Lewy bodies and Alzheimer's disease: an arterial spin labeling MRI study on prodromal and mild dementia stages. *Alzheimers Res Ther* 2016;8:29.
 54. Alsop DC, Casement M, de Bazelaire C, et al. Hippocampal hyperperfusion in Alzheimer's disease. *NeuroImage* 2008;42:1267–1274.
 55. Park D, Reuter-Lorenz P. The adaptive brain: aging and neurocognitive scaffolding. *Annu Rev Psychol* 2009;60:173–196.
 56. Persson J, Nyberg L. Altered brain activity in healthy seniors: what does it mean? *Prog Brain Res* 2006;157(06):44–57.
 57. Selden NR, Gitelman DR, Salamon-Murayama N, et al. Trajectories of cholinergic pathways within the cerebral hemispheres of the human brain. *Brain* 1998;121(12):2249–2257.
 58. Sridharan D, Levitin DJ, Menon V. A critical role for the right fronto-insular cortex in switching between central-executive and default-mode networks. *Proc Natl Acad Sci USA* 2008;105:12569–12574.
 59. Menon V, Uddin LQ. Saliency, switching, attention and control: a network model of insula function. *Brain Struct Funct*. 2010;214:655–667.
 60. Liang X, Zou Q, He Y, et al. Topologically reorganized connectivity architecture of default-mode, executive-control, and salience networks across working memory task loads. *Cereb Cortex* 2016;26(4):1501–1511.
 61. Naqvi NH, Bechara A. The insula and drug addiction: an interoceptive view of pleasure, urges, and decision-making. *Brain Struct Funct* 2010;214:435–450.
 62. Guo X, Han Y, Chen K, et al. Mapping joint grey and white matter reductions in Alzheimer's disease using joint independent component analysis. *Neurosci Lett* 2012;531:136–141.
 63. Lin F, Ren P, Lo RY, et al. Insula and inferior frontal Gyrus' activities protect memory performance Against Alzheimer's disease pathology in old age. *J Alzheimers Dis* 2017;55:669–678.
 64. Liu X, Chen X, Zheng W, et al. Altered functional connectivity of insular subregions in Alzheimer's disease. *Front Aging Neurosci* 2018;10:107.
 65. Xie C, Bai F, Yu H, et al. Abnormal insula functional network is associated with episodic memory decline in amnesic mild cognitive impairment. *NeuroImage* 2012;63:320–327.
 66. Braak H, Alafuzoff I, Arzberger T, et al. Staging of Alzheimer disease-associated neurofibrillary pathology using paraffin sections and immunocytochemistry. *Acta Neuropathol* 2006;112:389–404.
 67. Wang L, Wei Q, Wang C, et al. Altered functional connectivity patterns of insular subregions in major depressive disorder after electroconvulsive therapy. *Brain Imaging Behav* 2020;14(3):753–761. <https://doi.org/10.1007/s11682-018-0013-z>. [Online ahead of print].
 68. Wang C, Wu H, Chen F, et al. Disrupted functional connectivity patterns of the insula subregions in drug-free major depressive disorder. *J Affect Disord* 2018;234:297–304.
 69. Shelley BP, Trimble MR. The insular lobe of Reil-its anatomico-functional, behavioural and neuropsychiatric attributes in humans-a review. *World J Biol Psychiatry* 2004;5:176–200.
 70. Nieuwenhuys R. The insular cortex: a review. *Prog Brain Res* 2012;195:123–163.
 71. He W, Liu D, Radua J, et al. Meta-analytic comparison between PIB-PET and FDG-PET results in Alzheimer's disease and MCI. *Cell Biochem Biophys* 2015;71:17–26.
 72. Zhao Z, Fan F, Lu J, et al. Changes of gray matter volume and amplitude of low-frequency oscillations in amnesic MCI: an integrative multi-modal MRI study. *Acta Radiol* 2015;56:614–621.
 73. Thomann PA, Schäfer C, Seidl U, et al. The cerebellum in mild cognitive impairment and Alzheimer's disease—a structural MRI study. *J Psychiatr Res* 2008;42:1198–1202.
 74. Bas O, Acer N, Mas N, et al. Stereological evaluation of the volume and volume fraction of intracranial structures in magnetic resonance images of patients with Alzheimer's disease. *Ann Anat* 2009;191:186–195.
 75. Hauser T, Schönknecht P, Thomann PA, et al. Regional cerebral perfusion alterations in patients with mild cognitive impairment and Alzheimer disease using dynamic susceptibility contrast MRI. *Acad Radiol* 2013;20:705–711.
 76. Zhang Z, Liu Y, Zhou B, et al. Altered functional connectivity of the marginal division in Alzheimer's disease. *Curr Alzheimer Res* 2014;11:145–155.
 77. Zheng W, Liu X, Song H, et al. Altered functional connectivity of cognitive-related cerebellar subregions in Alzheimer's disease. *Front Aging Neurosci* 2017;9:143.
 78. Kaufmann L, Ischebeck A, Weiss E, et al. An fMRI study of the numerical stroop task in individuals with and without minimal cognitive impairment. *Cortex* 2008;44:1248–1255.